3

Adaptive Bend-Torsional Coupling Wind Turbine Blade Design Imitating the Topology Structure of Natural Plant Leaves

Wangyu Liu and Jiaxing Gong
South China University of Technology
China

1. Introduction

In the wind turbine system, the size of the blade is determined by the level of single output power. With the rise of offshore wind turbines (Breton & Moe, 2009), the output power of commercial blade has reached 5MW, and the length of the blade is over 100m. The design and manufacture limit of large-scale wind turbine is facing severe challenges, and as a result, wind turbine blade has become a research focus of scholars from all over the world. In a poor working environment, the problems of large blades in the following two aspects, which occur in the process of operation, will become more and more prominent.

1. In the operation, the blade should bear a good rigidity in order to minimize the destruction that random wind load and gust may cause to the blade (Bishop et al, 1999). Knut (1999) points out that due to the increasing length of wind turbine blade, the blade becomes more vulnerable to the unpredictable destruction caused by random gusts and ultimate wind load. And since the fatigue test of the blade has its limitations, therefore, he proposed a kind of random probability model based on bad working conditions to predict the fatigue life and reliability of the series of blades (Ronold & Larsen, 2000). Christoph (2006) points out that the length and weight of large-scale blade have an increasing impact on the bending load withstood internally. Meanwhile, it becomes more and more difficult for the large blades, which are subjected to wind, rain, moisture, and other adverse environmental effects, to meet the design requirements of a 20-year basic fatigue life. In order to predict the fatigue life of blade more accurately, apart from the unidirectional fiber, he has also made some research on the S-N curve of the off-axis fiber which bears the shear load. In addition, the research on the blade fatigue and damage mechanism has also been attached importance to by domestic and foreign researchers. For example, Daniel (2008), Raif (2008) and other scholars have delved into the fatigue and destruction data and the interlayer destruction mechanism of glass fiber and carbon fiber. They point out that both the technology of blade fiber manufacture and the adaptability of the blade have an important impact on the fatigue and destruction of the blade.

   Thus with the wind turbine blade becoming lager and larger, it becomes more and more difficult to maintain the rigidity of the blade. Even within the rated wind speed, the instability of the wind speed produces a serious varied load to the blade, increasing the

possibility of cyclic fatigue damage of the blade. When subjected to gusts or ultimate wind load, the blade, failing to adapt to the change immediately, becomes more vulnerable to invalid breakage, and thus its fatigue life is reduced. Therefore, it is very important to increase the blade flexibility as well as to improve its unloading effects.

2. The longer the blade is, the higher the tower holder is, and the more unstable the direction of the wind speed will be. As a result, the attack angle of the blade will vary in accordance with the change of the wind speed more easily, which in turn results in the increase of the instability of the power output. At the same time, with the increase of the blade cost, to increase wind turbine efficiency in order to lower the cost of wind power by designing adaptive blade has become the research focus (Lobitz & Veers,1999).

   As mentioned above, thus to reduce the impact of the instability of wind speed such as gusts on the blade, to improve the reliability and antifatigue merits of the large-scale blade as well as the stability of power output, and to broaden the scope of running wind speed have become the research hotspots that the current wind power field is concerned about. The existing technology is to improve the stability (Bao et al.,2007; Lin,2005) of the power output of the wind turbine blade by stalling, varying pitch angle and other methods, and some researchers also try to realize this in the ultra-large blade by reducing the area of the blade trailing edge strip (Lackner & Kuik, 2010). However, for those blades which are similar to slender cantilever beam, when the wind load is not fixed and the inertia force becomes larger and larger, the blade structure and the instability of the power output can hardly be regulated and controlled by the electromechanical system. And the feedback effect and the governing response speed can not meet the requirements of real-time control. As a result, the cost will increase accordingly. Therefore, to improve the adaptivity of the blade and reduce the reliance on the control system to achieve the stability of output power can meanwhile enhance the unloading function of the blade and improve its fatigue life, which is thus of research value.

2. Review of the development of adaptive blade

In fact, the tailorability and designability of the composite aeroelasticity has long been widely used (Büter & Breitbach, 2000) in the military and aviation fields, etc. Till 1990s, relevant researchers had begun to try to develop an intelligent blade which bears a good adaptability to the wind load from outside by designing a laminated blade material. Karaolis and other researchers have realized the blade twisting and the coupling of the relevant acting force through the mirror symmetry laminated design of the FRP composite of small blades. That is to say, with the change of the acting force, the twist angle of each section of the blade will change accordingly thus to unload some force and control the power output (Jeronimidis & Musgrove, 1989) of the blade. Joose and others have designed a kind of structure in which axial tensile deformation and twist deformation are coupled to adjust the rotation angle of the blade tip, and have analyzed the stability of power output and its protective capability for the blade in the cases of over-rated wind speed. DON (Lobitz & Veers, 1999) discussed about the tension, shear and twist coupling algorithm of the linear beam units and verified it through a set of combined experiments, figuring out the coupling factors of the blade tip in different twist angles. They have done a preliminary research on the contribution (Joosse et al., 1996) of coupling factors to the stability of the power. Andrew for the first time applied twist coupling effect design to the 50kW blade

systematically, and proposed a design idea of intelligent blade to enhance the blade's power control and lower the blade's fatigue loss (Andrew et al.,1999). So far, the blade with twist coupling effect is still at the stage of preliminary design, with some verifying experiments on some small blades.

Till early 21th century, as great importance had been attached to renewable energy by the countries all over the world, technology of wind power generation and the blade design theory has been developed rapidly. Researchers in this field have reached a common view to design an intelligent blade that bears a good adaptability to the bad environment. The Sandia National Laboratories of the United States had also begun to do some independent research as well as to fund developing the adaptive blade with torsion coupling property.

Don applied torsion coupling design to medium-sized blades of 300kW, and proved in detail in his report that adaptive blades are improved blades in terms of wind capturing efficiency, which are therefore able to increase the annual wind power catch. Although in the case of stalling, the chances of fatigue and destruction may be increased for adaptive blades, in the process of operation, its antifatigue property (Lobitz et al., 2001) is actually increased. Due to the complexity of the structure and the shape of wind turbine blade, it is difficult to obtain an accurate solution to the mechanical problem of wind turbine structure by applying the normal numerical analysis theory. However, with the maturity of the finite element analysis technology, it is also widely applied in the mechanical calculation of wind turbine blade structure. For instance, Ladean attains the bending stiffness and the shearing rigidity of the blade through the finite element technology, and also gains the static and dynamic mechanical property and the buckling frequency (McKittrick et al., 2001) under the circumstance of rated wind speed and ultimate wind load, which is of great reference value for further study.

The increase of the size of the blade calls for some material better than glass fibers which can now hardly meet the requirements of structure reliability. While carbon fibers, with its light weight and good comprehensive mechanical property, have become the first choice to replace glass fiber. In recent years, some scholars are dedicated to the study (Griffin & Ashwill, 2003) of the hybrid fibers mixed by glass fibers and carbon fibers, and have applied (Mohamed & Wetzel, 2006) them to the large scale commercial blade constantly. However, in terms of the hybrid fibers, there is still a problem of manufacture and cost constraints. And due to the complexity of the mechanism of fracture of the composite material itself, it will certainly be more difficult to predict and grasp the failure mode of hybrid fibers. In order to better grasp the fatigue and destruction mechanism of the hybrid fibers, John has made about 10^{10} experimental research on the fatigue property and strength reliability of different glass fibers and hybrid fibers samples in different stress ratio, which provides a good reference for the fracture mechanism of the fibers. The research results show that sewed epoxy hybrid fibers is better than the knitted hybrid fibers in terms of compression ratio intensity and antifatigue property (Mandell et al., 2003). Don (2001), under fatigue load, delves into the interlayer destruction mechanism of the hybrid fibers of glass fibers with variable cross-section and carbon fibers, and the result shows that interlayer stress and strain have great impact on the destruction of the fiber layer. Compared with glass fibers, under the maximum stress and strain in the bottom layer, carbon fibers are more susceptible to interlayer separation failure. Selwin used the finite element method to analyze the cause for the fatigue failure of the broken blade, and discovered that the estimated results agreed with the improved fatigue failure criteria (Rajadurai et al., 2008), which applies to all kinds

of composite materials. This provides a good reference for the optimization design of the wind turbine material. James, based on the NPS blade model, has introduced carbon fibers to the torsion coupling design of the blade, and established the model of the torsion coupling design of hybrid fibers. He has also checked the static and dynamic property under the ultimate load, and compared it with standard glass fibers blade, proving the advantages and feasibility (Locke & Valencia, 2004) of applying hybrid carbon fibers to the torsion coupling design.

In recent years, researchers have begun to apply torsion coupling design to the large scale blade. Dayton has begun to apply torsion coupling design to a large blade of 1.5Mw, and has studied the airfoil design of adaptive blade. At last he chose an off-axis skin airfoil, and evaluated it from the aspect of coupling effect. The results show that although the blade airfoil he designed has the potential (Griffin, 2004) to be manufactured as large scale adaptive blade, in his documents, due to the restrictions on the using of hybrid fibers considering cost and manufacture factors, he has only considered to use the hybrid fibers of the combination of 20° and 70°, which in turn makes it difficult to design an adaptive blade with optimal coupling effect. Based on this, Kyle put all off-axis carbon fibers in the beam cap of a long blade of 1.5MW, and used parametric methods to analyze the influence of different angles and volume ratios of the offset fibers on the torsion coupling effect. He proposed to optimally analyze the offset fiber angel (Wetzel, 2005) in which the optimal coupling effect of the blade occurs considering the stress, strain, and in-plane stress and strain as well as other comprehensive evaluation factors of the cross fibers of the blade. But Kyle also put too much emphasis on the cost of the blade manufacture, and ignored the possibility of balancing the cost through the improved power and fatigue property.

With the maturity of the design technology of torsion coupling blade, Alireza and other researchers have developed a comprehensive procedure combining aerodynamics and the coupling of the blade structure to accurately predict the angle of attack and bending moment of the adaptive blade during the process of design as well as the output power (Maheri et al., 2006; Maheri et al., 2007), which has reduced the heavy finite element calculation task in the process of optimization design thus saving the time and efforts in calculation. After that, they soon started to develop a set of design tools (Maheri & Isikveren, 2009a, 2009b) of adaptive blade. This procedure has applied the aerodynamic - structure iteration coupling algorithm, and is able to design an intelligent blade in which the maximum annual wind power capturing is realized through the alteration of the coupling design factors in different wind speeds according to the requirements of designers. This design procedure is still in the research stage, and has great reference value.

Some researchers, for example, Rachel (2007) and Nicholls-Lee (2009) have even applied the torsion coupling design idea of wind turbine to the design of tidal turbine blade as to improve the annual power capturing capability of the tidal turbine, approaching the Betz limit. The research shows that the adaptive blades of tidal power generation can also improve the annual power capturing capability, as well as reduce the load-carrying capability to enhance the reliability of the blade.

3. Bionic research of wind turbine blade

Martin Ryle, astronomer of Cambridge University, Nobel Prize winner, had predicted that if the blades can work like the palm tree in high wind speed, then the energy conversion efficiency can be increased by 50%, and the material can be saved by 2/3 (Platts & Liu,

2008). Ryle thus had tried to study the flexible wind turbine. As early as in the early 80s of last century, the concept of flexible wind turbine has aroused great attention, and small wind turbines represented by Carter flexible wind turbine have been developed and put into use. However, since the traditional theory applied to the wind turbine design is no longer suitable for the flexible wind turbine in which the plane of rotation has changed, at that time the research and development of small flexible wind turbine mainly adopted the trial and error method. As the wind turbine is developed towards the tendency of large size, the trial and error method is no longer suitable for the development of large equipments. And flexible wind turbine, due to its inadequacy in the reliable design theory, was a mere flash in the pan, failing to become the mainstream of the development of wind turbine. Nevertheless, flexible wind rotor, due to its excellent cost performance and the wide adaptability to wind load changes, is still the research field that some scholars would like to devote their whole life to. In the 90s of the 20th century, Peter Jamieson, British engineer, proposed the concept of coning blade, and conducted some fruitful research, gaining the relevant aerodynamic performance curves of coning blade. The results show that compared with conventional design, using the wind blade with the same length, the minimum start-up wind speed can be decreased from 4m/s to 3m/s, and the ability to withstand hurricanes can reach 70m/s. A research team led by Jim Platts of Cambridge University, based on the research of Peter Jamieson, established a BEM coning blade theory based on trimming and revision. In the theory, articulated juncture method is adopted to control the open and close of the wind blade, so as to adjust the solidity of the wind blade to control the output power. In this way, the complete performance curve of the coning blade is gained, the power capture coefficiency of wind power is increased, and the cost of wind power generation is lowered (Curran & Platts, 2006; Curran, 2006).

Sarikaya (1990) and Gordon (1980) have delved into biological composite materials and its bionic application, and both of them believe that the organisms have optimized their structure, shape and function after a long-term evolution of hundreds of millions of years in the natural environment. Steele, Somerville and other scholars have verified that there is a necessary connection (Steele, 2006; Chris et al., 2004) between the production of the biological shape and tissue and the environmental stress. The research of Jones and others shows that the optimization results of biological tissues present Michell's truss topological structure, and match trajectory of principal stress (Jones & Platts, 1998). Medial axis exists in a lot of organisms (Blum & Nagel, 1978) as an optimized pattern, such as the common vein tissues or grass tissues, as well as the skeleton structure of many animals. There must be some links between the pattern and structure and the growth of the organisms.

In recent years, the author's group is mainly devoted to the research on the enhancement mechanism (Liu & Hou, 2007; Liu et al., 2009) of the topological structure of plant leaves. The research shows that the mesophyll of the leaves and the marrow in the skeleton form a multiphase and natural composite structure, and the medial axis network undoubtedly bears the function of enhancing the tissues. Therefore, in order to explore the mechanical enhancement mechanism of the leaf skeleton on the part of the topological structure of plant leaves, some experimental studies and numerical simulations on many groups of leaf samples were carried out. The analysis shows that the plant leaf can always maintain relatively smaller internal strain energy. According to the topological graph of plant leaves in single load field and multi-load field, stress is one of the inducing factors for vein growth, and apart from the realization of its physiological function, vein distribution, in order to adapt to the changes of the complicated environmental stress, its network has evolved into a

stable and adaptive medial axis structure. Subsequently, our study again focuses on the wind resistant plants in the coastal area, for example, the palm tree series. The study finds that palm tree trunks and branches are the natural fibrous composite which forms a good system combining rigidity and flexibility. And the leaves also bear a good flexible property. From our point of view, this is not only related to the flexible structure of itself, but also has some links with its material structure, which bears good rigidity, strength, and toughness.

3.1 The bend-torsion coupling design of wind turbine blade

3.1.1 Blade material and coupling effect

3.1.1.1 Composite blade

In recent decades, high performance composite material develops rapidly. The typical composite material are glass fibers reinforced polymers and carbon fibers, which are widely applied in engineering. The advantages of composites are (Jiang et al., 1990):

1. High ratio strength and stiffness, which means stronger and stiffer with the same mass.
2. Good fatigue performance.
3. Design ability, which means the engineer can customize the performances of the composite products.
4. High safety coefficient.

In wind turbine machine, the turbine blade is the key structural component. Therefore, reasonable structure, superior and light material, advanced manufacturing technique and etc must be required for the blade to withstand the adverse stress environment, such as the bend and torsion moment, the pulling force induced by the wind load, the gravity and inertial force. Composites material becomes the first choice owning to its advanced performances mentioned above. Currently, hybrid composites, mixed with glass/carbon fiber reinforced polymers, are utilized in large-scale wind turbine blade. With the increase of blade size, more carbon fiber reinforced composites are used in order to reduce the weight and raise its reliability.

3.1.1.2 Fundamentals of the layering theory of composite laminate

The turbine blade is manufactured by composite layering technique. As the good designable characteristic of fiber reinforced composites, some complex coupling effect, such as tensile-shear, bend-torsion, can be achieved through composite layering method. The following section will give a brief introduction to the coupling design of composite laminates. The context of this part can be found in many textbooks (Jiang et al., 1990).

Laminate is made up of unidirectional thin plates layered according to the designed sequence and angles. In order to evaluate the laminate stiffness, the following hypothesis is made:

1. Made-in-art bond strength and no gap between layers, discounting the thickness of the bond layer.
2. The thickness is very small, and the line perpendicular to the middle plane keeps its shape and position (perpendicular to the middle plane) after deformation.

The stress in the *kth* layer can be represented as,

$$\begin{bmatrix} \sigma_x \\ \sigma_y \\ \tau_{xy} \end{bmatrix}_k = \begin{bmatrix} \overline{Q_{11}} & \overline{Q_{12}} & \overline{Q_{16}} \\ & \overline{Q_{22}} & \overline{Q_{26}} \\ sym. & & \overline{Q_{66}} \end{bmatrix}_k \left\{ \begin{bmatrix} \xi_x^0 \\ \xi_y^0 \\ \gamma_{xy}^0 \end{bmatrix} + z \begin{bmatrix} K_x \\ K_y \\ K_{xy} \end{bmatrix} \right\} \tag{1}$$

Where $[Q]_k$ is the stiffness matrix of layer *k*, *z* is the coordinate variable in the direction of thickness. ξ_x^0, ξ_y^0, γ_{xy}^0 are the normal and shear strain in the middle plane of the laminate, K_x, K_y, K_{xy} are the bend and torsion curvatures, respectively. *Sym* means the elements in the matrix is symmetrical to the main diagonal elements. If the displacement of the middle plane are μ_0, ν_0, ω_0, then

$$\begin{bmatrix} \xi_x^0 \\ \xi_y^0 \\ \gamma_{xy}^0 \end{bmatrix} = \begin{bmatrix} \frac{\partial_{\mu 0}}{\partial x} \\ \frac{\partial_{\nu 0}}{\partial y} \\ \frac{\partial_{\mu 0}}{\partial x} + \frac{\partial_{\nu 0}}{\partial y} \end{bmatrix}; \begin{bmatrix} K_x \\ K_y \\ K_{xy} \end{bmatrix} = \begin{bmatrix} -\frac{\partial^2 \omega_0}{\partial x^2} \\ -\frac{\partial^2 \omega_0}{\partial y^2} \\ -2\frac{\partial^2 \omega_0}{\partial x \partial y} \end{bmatrix} \tag{2}$$

Suppose the resultant inner force per unit of the laminate are N_x (pulling force), N_y (compressive force), and N_{xy} (shear force), and the resultant inner moment (bend or torsion moment) are M_x, M_u and M_{xu}, shown as Fig.1 and Fig.2.

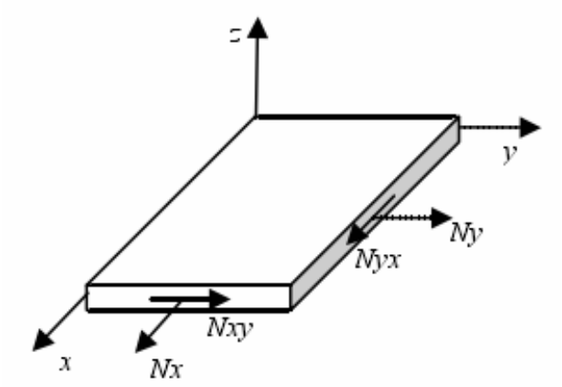

Fig. 1. The resultant inner force

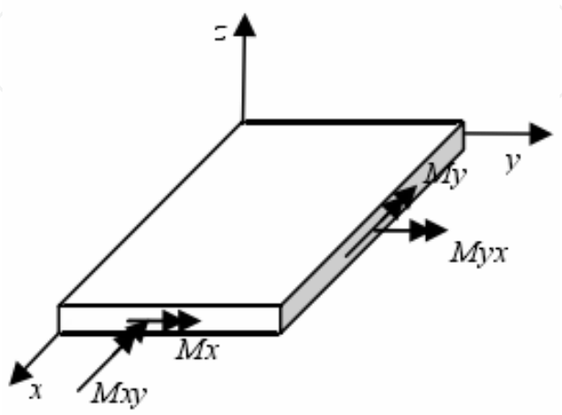

Fig. 2. The resultant inner moment

The constituent equations of the laminate are,

$$\begin{bmatrix} N_x \\ N_y \\ N_{xy} \end{bmatrix}_k = \begin{bmatrix} A_{11} & A_{12} & A_{16} \\ & A_{22} & A_{26} \\ sym. & & A_{66} \end{bmatrix} \begin{bmatrix} \xi_x^0 \\ \xi_y^0 \\ \gamma_{xy}^0 \end{bmatrix} + \begin{bmatrix} B_{11} & B_{12} & B_{16} \\ & B_{22} & B_{26} \\ sym. & & B_{66} \end{bmatrix} \begin{bmatrix} K_x \\ K_y \\ K_{xy} \end{bmatrix} \tag{3}$$

$$\begin{bmatrix} M_x \\ M_y \\ M_{xy} \end{bmatrix}_k = \begin{bmatrix} B_{11} & B_{12} & B_{16} \\ & B_{22} & B_{26} \\ sym. & & B_{66} \end{bmatrix} \begin{bmatrix} \xi_x^0 \\ \xi_y^0 \\ \gamma_{xy}^0 \end{bmatrix} + \begin{bmatrix} D_{11} & D_{12} & D_{16} \\ & D_{22} & D_{26} \\ sym. & & D_{66} \end{bmatrix} \begin{bmatrix} K_x \\ K_y \\ K_{xy} \end{bmatrix} \tag{4}$$

$$A_{ij} = \int_{-\frac{h}{2}}^{\frac{h}{2}} Q_{ij} dz \,,\; B_{ij} = \int_{-\frac{h}{2}}^{\frac{h}{2}} Q_{ij} dz \,,\; D_{ij} = \int_{-\frac{h}{2}}^{\frac{h}{2}} Q_{ij} dz \tag{5}$$

In equation (5), A_{ij} are the stiffness coefficients between the stress and middle plane strain, called as the pulling stiffness; D_{ij} are the stiffness coefficients related with the inner moment, the curvature, and torsion curvature, generally called as flexural stiffness; B_{ij} is a coefficient not only coupled with the pulling deformation but also with the flexure, generally called as the coupling stiffness. When the layer of the laminate is decided, all the stiffness mentioned can be calculated in the first place, then the stress and strain analysis can be carried out.

It can be observed from formula (3) and (4) that the in-plane inner force in the laminate will result in flexural deformation (bend and torsion), and the flexural inner force (bend and torsion moment) will result in the in-plane deformation, which are called the coupling effect of pulling and flexure. The complicated physical relationship of laminate can be explained from the coupling stiffness matrix B. Matrix A denotes the coupling effect of pulling and shearing, and matrix D gives the coupling effect of bend and torsion. In adaptive wind turbine blade design, the main task is to design proper matrix D to realize the adaptive coupling of bend and torsion.

The performances of composites not only relate with the matrix and reinforced material, but also with the fibers volume ratio and arrangement. The stiffness of the laminate can be designed by changing the fibers arrangement. Their relation is shown in table 1, where the definition of the layer specification can be found in literatures about composites mechanics.

It can be found from Table 1 that, in order to achieve the bend-torsion coupling effect given by matrix D and avoid the influence of coupling matrix B, the off-axis fiber arrangement in symmetrical means must be followed.

3.1.2 Example validation of coupling design

In this section, a simple example is taken to verify the bend-torsion coupling effect of the theory mentioned above, and to provide evidence for the following computing method. Supposing that there is a piece of simple laminated plate with 10m length, 1m width and 30 layers, 10mm thickness of each layer. The material property is shown as the followings: axial modulus $E_x = 36.47\text{GPa}$, radial modulus E_y=12.6GP$_a$, poisson ratio U_x=0.22, shear modulus G_{xy}=3.94GPa. Fix the root and put a concentrated force, F=10KN, at the midpoint of the end.

stiffness		Pulling stiffness	Coupling stiffness	Flexural stiffness
Symmetrical arrangement	Normal isotropic inhomogeneous	$A_{ij} \neq 0$	0	$D_{ij} \neq 0$
	Special isotropic inhomogeneous	$A_{16} \neq 0$ $A_{26} \neq 0$	0	$D_{16} \neq 0$ $D_{25} \neq 0$
	Off-axis arrangement	$A_{ij} \neq 0$	0	$D_{ij} \neq 0$
Anti-symmetrical arrangement	Isotropic arrangement	$A_{11} = A_{12}$ $A_{16} = A_{26} = 0$	$B_{22} = -B_{11}$ the other $B_{ij} = 0$	$D_{11} = D_{12}$ $D_{16} = D_{26} = 0$
	Off-axis arrangement	$A_{16} = 0$ $A_{26} = 0$	$B_{16} \neq 0$ and $B_{26} \neq 0$ the other $B_{ij} = 0$	$D_{16} = 0$ $D_{26} = 0$
Non-symmetrical arrangement	Normal isotropic inhomogeneous	$A_{ij} \neq 0$	$B_{ij} \neq 0$	$D_{ij} \neq 0$
	Special isotropic inhomogeneous	$A_{16} = 0$ $A_{26} = 0$	$B_{16} = 0$ $B_{26} = 0$	$D_{16} = 0$ $D_{26} = 0$
Bi-unidirectional		$A_{16} = 0$ $A_{26} = 0$	$B_{16} = 0$ $B_{26} = 0$	$D_{16} = 0$ $D_{26} = 0$

Table 1. The stiffness of different fiber arrangement

Theoretical method is firstly used to deduce the stress and strain of the laminated plate, and then finite element method is carried out to verify the correctness of the computing method. Supposing that the laminate plate is unidirectional and the fiber placement follows the lengthwise direction of the plate. As the laminated plate is in regular shape, the length, width and height are l=10m, b=1m, h=0.3m respectively. The laminated plate could be equivalent to a beam, and the root of which is fixed. According to the beam theory, the bend moment at the beam root is,

$$M_{\max} = F \times l = 100000N.m$$

The bend inertial moment of the beam is,

$$W = \frac{b * h^2}{6} = \frac{1 \times 0.3 \times 0.3}{6} = 0.015 \ m^3$$

Then the maximum tensile stress at the root is,

$$\sigma_{\max} = \frac{M_{\max}}{W} = \frac{100000}{0.015} = 66.7 \text{ MPa}$$

The strain is,

$$\xi_x = \frac{\sigma_{\max}}{Ex} = 0.00183$$

Use finite element method to solve the problem. Fig.3 and Fig.4 show the results. The root average tensile stress is about 67MPa, and the maximum strain is 0.00187, which is close to the result with beam theory method.

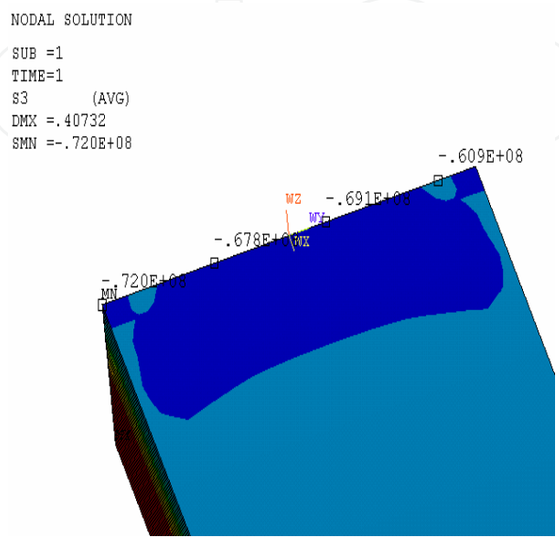

Fig. 3. Tensile stress at root

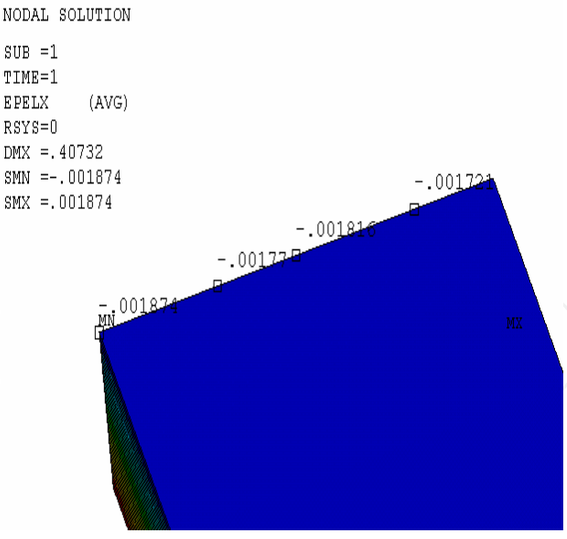

Fig. 4. Compressive strain at root

The following content takes the laminated plate for an example to discuss the coupling effect of the laminated plate. Firstly, under the unidirectional layer condition mentioned above, the result of the displacement of the laminated plate end is shown in Fig.5. It can be seen that the displacement of the two end-points is equal, and no torsion displacement happens. However, when the layer pattern is changed into angular layer, for example, the

fibers are in 20° off the lengthwise direction, the torsion deflection, say 2.73° drawn from the result, will be achieved shown as Fig.6. In the context, a group of off-axis fibers placed in different angles among 0°~40°, could make the similar bend-torsion coupling effect.

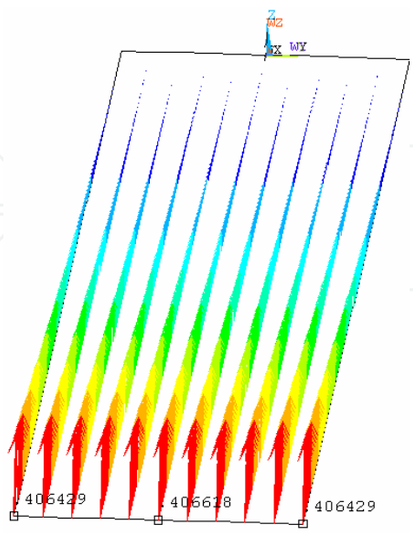

Fig. 5. End displacement of unidirectional laminated plate

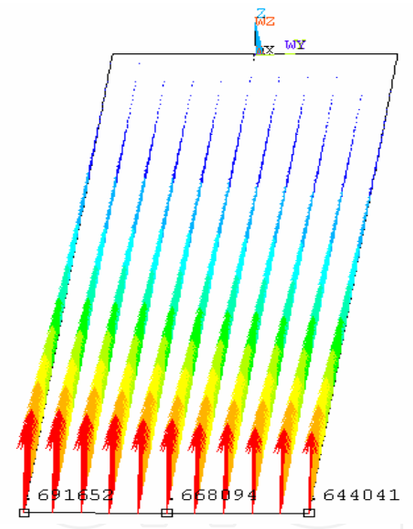

Fig. 6. End displacement of off-axis laminated plate

It can be seen from the example mentioned above, when the layer angle of the fiber in the laminated plate does not deviate from the coordinate axis, no coupling effect would be achieved. And when it does, the bend-torsion coupling effect would be generated. It just verifies that the bend-torsion coupling theory of laminated plate is correct, and it is reasonable and accurate to use finite element method to calculate the coupling effect.

3.1.3 The layer and coupling effect in blade

The coupling design method of composite laminate is widely used in several fields, for example, the aviation. While in the wind turbine machine design, the designers usually try

to eliminate the coupling effect caused by the blade layer. Traditionally, unidirectional fibers (0°) and ±45° triaxial fibers are used in blade layering. With the increase of the blade size, coupling design of the blade shows potential advantages in some aspects. According to previous content, laminated plate with off-axis fibers placement would achieve favorable bend-torsion coupling effect. Whereas, in wind turbine blade design, it would work well if the fibers are placed in mirror way (not 0°) in the coupling area of the two chord faces up and down, shown as Fig.10. Where, θ means the off-axis angle.

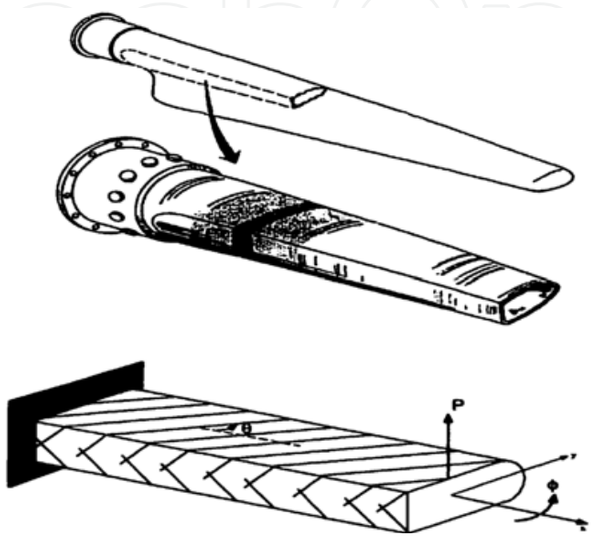

Fig. 7. Bend-torsion coupling design method in the blade spar (Ong, 2000)

3.1.3.1 The control of coupling ratio

In finite element, the 3-D beam element provides an efficient and short-cut computing method for the coupling effect design. In order to analyze the coupling effect of fiber layer more accurately, Cheng conducts two part of modification to beam element theory (Cheng, 2000), (1) Considering about the in-plane lateral shear stress and strain; (2) Considering about the out-of-plane bending effect relative to torsion, and conducting intensive study on the bend-torsion coupling effect through theory analysis.

The bend-torsion coupling effect of wind turbine blade is realized through the laminate layer design method to achieve the stiffness D mentioned above, and at the same time, certain torsion effect could be achieved when the blade bends. Whereas, how to evaluate the coupling effect with a parameter indicator? Kyle. K Wetzel. (Wetzel, 2005) have made much investigations. Carried on his work and based on cantilever beam theory, the authors made some calculations for the selected blade model.. Since the blade spar is usually made up with symmetrical section, it is equal to the cantilever beam of symmetric distribution. Its bend-torsion coupling control equation is,

$$\begin{bmatrix} EI & -K \\ -K & GJ \end{bmatrix} \begin{bmatrix} \dfrac{\partial \theta}{\partial z} \\ \dfrac{\partial \varphi}{\partial z} \end{bmatrix} = \begin{bmatrix} M_b \\ M_t \end{bmatrix} \tag{6}$$

In the equation above: EI is the bending stiffness in the blade flapping direction; GJ is the torsion stiffness in the blade spanwise direction; K is the coupling term; θ is the bend angle

of the cross section; φ is the torsion angle; M_b is bending moment of the cross section; M_t is the torsional moment of the cross section.
According to equation(6)：

$$EI * GI\frac{\partial\theta}{\partial z} - K * GJ\frac{\partial\varphi}{\partial z} = M_b * GJ \tag{7}$$

$$-K^2\frac{\partial\theta}{\partial z} + K * GJ\frac{\partial\varphi}{\partial z} = M_t * K \tag{8}$$

Using the two equations above, it can be deduced that,

$$\frac{\partial\varphi}{\partial z} = \frac{M_b * K + M_t * EI}{EI * GJ - K^2};\ \frac{\partial\varphi}{\partial z} = \frac{M_b * GJ + M_t * K}{EI * GJ - K^2} \tag{9}$$

Supposing that the blade length is l, and there is a concentrated force working on the spar end. At the same time, the bending and torsional moment at any section x in spanwise direction are $M_b = F(l-x)$, $M_t = 0$. Substitute them into equation (9), an integral calculation is conducted on the equation above in the beam spanwise direction, and the bending deformation and torsion angle at section x can be obtained as the followings:

$$\theta = \frac{P(2lx - x^2)}{2(EI - K^2/GJ)} \tag{10}$$

$$\varphi = \frac{P * K(2lx - x^2)}{2(EI * GJ - K^2)} \tag{11}$$

Then the maximum torsion angle at the blade tip is:

$$\varphi_l = \frac{FKl^2}{2(\mathrm{EI} * \mathrm{GJ}\text{-}\mathrm{K}^2)} \tag{12}$$

Now, supposing that:

$$\alpha^2 = \frac{K^2}{EI \bullet GJ} \tag{13}$$

Substitute equation (13) into equation (12), then

$$\varphi_l = \frac{F\alpha l^2}{2\sqrt{\mathrm{EI} * \mathrm{GJ}}(1\text{-}\alpha^2)} = \frac{Fl^2}{2}\frac{1}{\sqrt{\mathrm{EI} * \mathrm{GJ}}}\frac{\alpha}{1\text{-}\alpha^2} \tag{14}$$

It can be seen from equation (13) and (14) that, when $\alpha/1\text{-}\alpha^2$ becomes the maximum, α tends to be 1 and $EI * GJ$ tends to be the minimum, and the biggest torsion angle at the blade tip would become the maximum. This demonstrates that, to get the biggest torsional deformation, $EI * GJ$ should be minimized, and α should be maximized. Here, α is called

as the blade coupling control ratio. The following section will give more details about the factors that affects α , and how the coupling ratio relates with the off-axis angle of the fibers.

3.1.3.2 The factors that affect the control ratio

1. Material factor

It is necessary to discuss the factors that affect coupling control ratio before designing the coupling airfoil profile of the blade. In this section, a 2-D composite plate is chosen as an example to make the explanation. The constitutive equations of material stress and strain is:

$$\begin{pmatrix} \sigma_x \\ \sigma_y \\ \tau_{xy} \end{pmatrix} = \begin{pmatrix} Q_{11} & Q_{12} & Q_{16} \\ Q_{21} & Q_{22} & Q_{26} \\ Q_{61} & Q_{62} & Q_{66} \end{pmatrix} \begin{pmatrix} \varepsilon_x \\ \varepsilon_y \\ \gamma_{xy} \end{pmatrix} \tag{15}$$

In the equation above: σ_i , τ_{ij} are tensile stress and shearing stress respectively; ε_i , γ_{ij} are tensile strain and shearing strain; When the material principal axis and the coordinate axis tend to be the same, Q_{ij} is the flexible ($S_{16} = S_{26} = S_{61} = S_{62} = 0$) component; When the material principal axis is deviated from the coordinate axis with an angle θ , S_{ij} is off-axis flexibility component.

Now resolve equation (15) into 3 terms,

$$\begin{cases} \sigma_x = Q_{11}\xi_x + Q_{12}\xi_y + Q_{16}\gamma_{xy} \\ \sigma_y = Q_{21}\xi_x + Q_{22}\xi_y + Q_{26}\gamma_{xy} \\ \sigma_x = Q_{61}\xi_x + Q_{62}\xi_y + Q_{66}\gamma_{xy} \end{cases} \tag{16}$$

Supposing that σ_y =0 in plane stress state, then,

$$\xi_y = -\frac{Q_{21}\varepsilon_x + Q_{26}\gamma_{xy}}{Q_{22}} \tag{17}$$

Substitute equation (17) into equation (16), and the following equations can be obtained,

$$\sigma_y = \left(Q_{11} - \frac{Q_{12} \bullet Q_{21}}{Q_{22}} \right) \xi_x + \left(Q_{16} - \frac{Q_{12} \bullet Q_{26}}{Q_{22}} \right) \gamma_{xy} \tag{18}$$

$$\tau_{xy} = \left(Q_{61} - \frac{Q_{62} \bullet Q_{21}}{Q_{22}} \right) \xi_x + \left(Q_{66} - \frac{Q_{62} \bullet Q_{26}}{Q_{22}} \right) \gamma_{xy} \tag{19}$$

Then turn the two equations above into matrix form:

$$\begin{pmatrix} \sigma_y \\ \tau_{xy} \end{pmatrix} = \begin{pmatrix} \overline{Q_{11}} & \overline{Q_{12}} \\ \overline{Q_{21}} & \overline{Q_{22}} \end{pmatrix} \begin{pmatrix} \xi_x \\ \gamma_{xy} \end{pmatrix} \tag{20}$$

Where,

$$\overline{Q_{11}} = Q_{11} - \frac{Q_{12}Q_{21}}{Q_{22}}$$

$$\overline{Q_{12}} = Q_{16} - \frac{Q_{12}Q_{26}}{Q_{22}}$$

$$\overline{Q_{21}} = Q_{61} - \frac{Q_{62}Q_{21}}{Q_{22}}$$

$$\overline{Q_{22}} = Q_{66} - \frac{Q_{62}Q_{26}}{Q_{22}}$$

And according to the classical composite laminate theory, the relationship among force, moment, stress and strain are,

$$\begin{pmatrix} \mathrm{N_x} \\ \mathrm{N_{xy}} \\ \mathrm{M_x} \\ \mathrm{M_{xy}} \end{pmatrix} = \begin{pmatrix} \overline{A_{11}} & \overline{A_{16}} & \overline{B_{11}} & \overline{B_{16}} \\ \overline{A_{61}} & \overline{A_{66}} & \overline{B_{61}} & \overline{B_{66}} \\ \overline{B_{11}} & \overline{B_{61}} & \overline{D_{11}} & \overline{D_{16}} \\ \overline{B_{16}} & \overline{B_{66}} & \overline{D_{61}} & \overline{D_{66}} \end{pmatrix} \begin{pmatrix} \xi_x^0 \\ \gamma_{xy}^0 \\ \kappa_x \\ \kappa_{xy} \end{pmatrix} \tag{21}$$

Where,

$$\overline{A_{ij}} = \int \overline{Q_{ij}} dz \; ; \; \overline{B_{ij}} = \int \overline{Q_{ij}} x dx \; ; \; \overline{D_{ij}} = \int \overline{Q_{ij}} x dx$$

ξ_x^0 , γ_{xy}^0 are the tensile stress and shearing strain of the middle plane, κ_x and κ_{xy} are the bending and torsional ratio of the middle plane, x is the vertical distance between the laminate and the middle plane. As to unidirectional laminated plate with symmetrical layer, equation (21) could be changed into:

$$\begin{pmatrix} \mathrm{N_x} \\ \mathrm{N_{xy}} \\ \mathrm{M_x} \\ \mathrm{M_{xy}} \end{pmatrix} = \begin{pmatrix} \overline{A_{11}} & \overline{A_{16}} & 0 & 0 \\ \overline{A_{61}} & \overline{A_{66}} & 0 & 0 \\ 0 & 0 & \overline{D_{11}} & \overline{D_{16}} \\ 0 & 0 & \overline{D_{61}} & \overline{D_{66}} \end{pmatrix} \begin{pmatrix} \xi_x^0 \\ \gamma_{xy}^0 \\ \kappa_x \\ \kappa_{xy} \end{pmatrix} \tag{22}$$

According to the equation above, only tensile-shear and bend-torsion coupling effect exist, which is as exactly as what is expected.

If dissymmetry layer method is used in laminate layer, the coupling effect would be more complicated. Equation (22) can be turned into the following form,

$$\begin{pmatrix} \mathrm{N_x} \\ \mathrm{N_{xy}} \\ \mathrm{M_x} \\ \mathrm{M_{xy}} \end{pmatrix} = \begin{pmatrix} \overline{A_{11}} & 0 & 0 & \overline{B_{16}} \\ 0 & \overline{A_{66}} & \overline{B_{61}} & 0 \\ 0 & \overline{B_{61}} & \overline{D_{11}} & 0 \\ \overline{B_{16}} & 0 & 0 & \overline{D_{66}} \end{pmatrix} \begin{pmatrix} \xi_x^0 \\ \gamma_{xy}^0 \\ \kappa_x \\ \kappa_{xy} \end{pmatrix} \tag{23}$$

According to equation (23), the laminated plate contains all of the coupling terms, and it is too complicated to control.
Because most of the blade spar of wind turbine machine is made up of unidirectional off-axis fibers, the coupling control ratio could be expressed as:

$$\alpha = \frac{-\overline{Q_{16}}}{\sqrt{\overline{D_{11}} \bullet \overline{D_{16}}}} \tag{24}$$

Substitute each terms of equation (20) into the equation above, then

$$\alpha = \frac{Q_{16} \bullet Q_{22} - Q_{12} \bullet Q_{26}}{\sqrt{(Q_{11} \bullet Q_{22} - Q_{16}^2) - (Q_{66} \bullet Q_{22} - Q_{26}^2)}} \tag{25}$$

$$\alpha^2 = \frac{(Q_{16} \bullet Q_{22} - Q_{12} \bullet Q_{26})^2}{(Q_{11} \bullet Q_{22} - Q_{16}^2) - (Q_{66} \bullet Q_{22} - Q_{26}^2)} \tag{26}$$

Define,

$$\nu_{16} = \frac{Q_{12} \bullet Q_{26} - Q_{16} \bullet Q_{22}}{Q_{11} \bullet Q_{22} - Q_{12}^2} \tag{27}$$

$$\nu_{61} = \frac{Q_{12} \bullet Q_{26} - Q_{16} \bullet Q_{22}}{Q_{66} \bullet Q_{22} - Q_{26}^2} \tag{28}$$

Then the coupling parameter equation could be simplified as:

$$\alpha = \sqrt{\frac{\nu_{16}}{\nu_{61}}} \tag{29}$$

So far, a simple equation through theory deduction of coupling control ratio is clear. According to equation (29), the coupling control ratio is only relative to Q_{ij} of the material, the layer flexible component of laminated plate. It means that the coupling ratio is only relative to the material itself and the layer angle.

2. Other factors

In theoretical calculation, a simplified model, say that a regular unidirectional one layer laminate plate with common modified beam theory, is chosen as the example to make the validation. Whereas, it is necessary to study the effect of other important factors, such as the geometry shape, material property, layer ratio and so on, on the coupling control ratio. Ong (1999) took composite materials spar of D-SPAR shape as an example, and analyzed the effect of several factors on the coupling ratio,

1. Geometry factor. Through the calculation of several samples of D-SPAR and aerofoil NACA0012, it was found that the coupling control ratio between the samples made little difference.
2. Layer factor. The layer factor mainly includes the effect of layer thickness and layer arrangement. The research showed that the layer thickness and layer material gave little influence on the coupling control ratio.

3. Fiber volume ratio. The coupling control ratio magnifies as the fiber volume ratio does.
4. Inner web stiffness. If the web is fixed inside the sample, its existence would increase the bending and torsional stiffness of the blade, which results in the reduction of coupling effect.
5. Layer method. There are several layer method of composite materials mentioned above, and wind turbine machines usually employ unidirectional and dissymmetrical laminate as the choice of fiber arrangement in composite. Moreover, mirror arrangement of fibers is necessary to provide bend-torsion coupling effect. As Fig.8(a) shows, the stiffness matrix from the layer is bend-torsion coupling stiffness and tensile-shear coupling stiffness. But if dissymmetry mirror layer arrangement is employed, as Fig.8(b) shows, the resultant stiffness matrix contains not only the bend-torsion coupling stiffness and tensile-shear stiffness, but also the tensile-shear-bend-torsion coupling stiffness, making the coupling behavior of the D-SPAR too complicated to control, as well as the coupling ratio of the laminated plate.

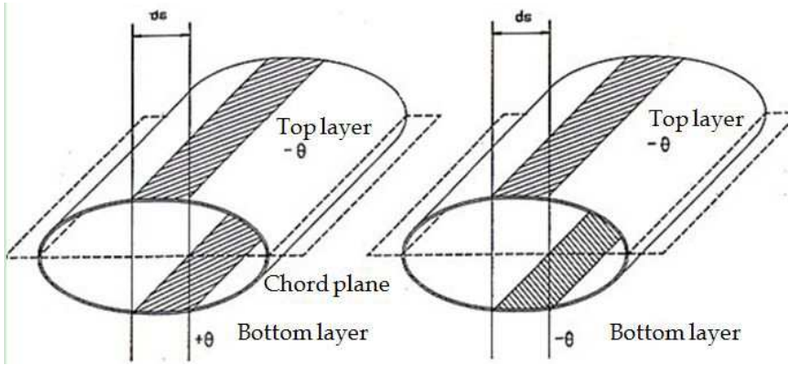

(a) Mirror symmetry layer (b) Dissymmetry layer

Fig. 8. Layer method

3.2 The adaptive blade design based on the compliant structure of plant leaf

Medial axis pattern is a general phenomenon almost for all biology, such as the plant leaf vein, the skeleton of creature observed from the macro-level. From the viewpoint of material science, the medial axis skeleton, combined with the other phase of the organism, formed a kind of composite structure with multiple phases. Obviously, the network of medial axis pattern takes the function of reinforcement (Gibson & Ashby, 1997). Whereas, how does this kind of topology structure adapt to the environmental stress? Does it have any meaning in guiding the structural design? In this section, we firstly achieved the mechanical performances of plant leaf vein through experiment, then the pattern evolution process from the viewpoint of topology optimization was carried out. Finally, a case study was given to validate the effect of bionic design methodology in wind turbine blade design.

3.2.1 The mechanical property and bionic study of compliant structure of plant leaf (Liu & Zhang, 2010a)

3.2.1.1 Sample preparation and measurement method

In order to explore the compliant structure and adaptability of the vein pattern of plant leaf, five fresh and mature leaf samples, which represent the typical leaf network in nature, are

collected. 6 samples, which are ficus altissima, pineapple, kemirinoten, madagascar palm, ficus viren, and royalplam are picked in the campus shown in Fig.9. Royalplam and madagascar palm are monocotyledons plants with parallel pulse, the others are dicotyledonous plants with network veins. Royalplam is one of the most wind resistant plant in offshore, whereas, ficus viren has poor ability in carrying high wind load. In addition to the different abilities in carrying loads, the 6 plants are also quite different in thickness, shape outline, leaf texture and vein distribution. Therefore, the samples chosen are typically representative.

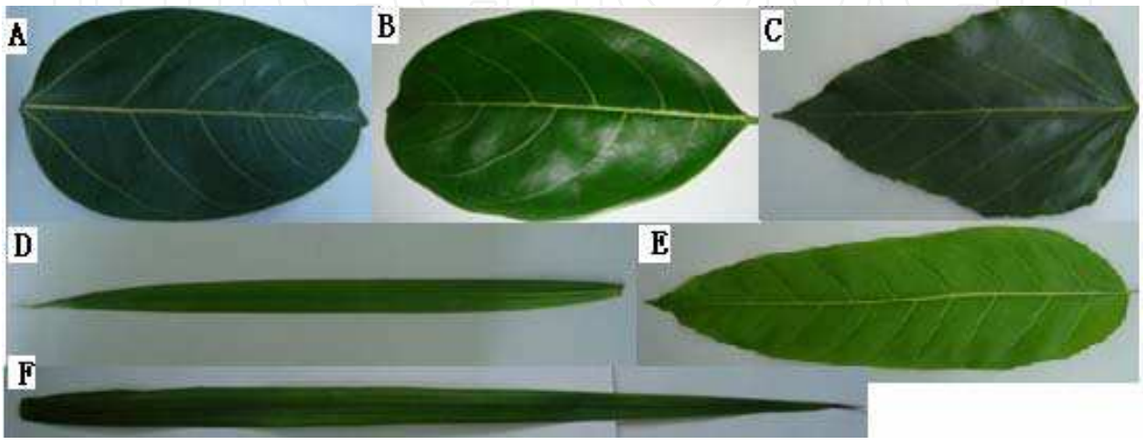

Fig. 9. The fresh plant leaf

For each kind of plants, 15 fresh samples with similar shape and size are collected. Firstly, a digimatic calliper is used to measure the leaf thickness. As the actual thickness of plants leaf is different from the root to the tip, the thickness measured was processed into an average value along the leaf spanwise direction. Secondly, in order to prevent the water loss of leaf from influencing the density result, the leaves with the polythene bags on are placed in the refrigerator, and keep the refrigerator temperature around 4℃. Before experiment, the leaves are wiped dry and each leaf mass is measured by using electronic balance with the accuracy of 0.001g. Finally, the mechanical performances are measured on a universal material tester in Fig.10, the results are shown in Table 2.

Fig. 10. The tension test of plant leaf

Property	Symbol	Ficus altissima	Pineapple	Kemirinoten	Ficus viren	Royalplam
Thickness	$T\ /\ mm$	0.43 ±0.023	0.37 ±0.029	0.29 ±0.016	0.17±0.019	0.25 ±0.029
Density	$\rho\ /\ kg\ /\ m^3$	55.87 ±7.63	63.05 ±19.44	40.23 ±5.11	703.9 ±37.4	0.25 ±0.029
Mesophyll modulu	$E_m\ /\ MP_a$	55.87 ±7.63	63.05 ±19.44	40.23 ±5.11	45.31 ±10.14	938 ±120.24
Leaf vein modulu	$E_v\ /\ MP_a$	229.7 ±55.13	199.9 ±35.85	157.6 ±28.70	99.8 ±33.82	4833 ±913.93
Possion ratio[13]	ν	0.33	0.33	0.33	0.33	0.33

Table 2. The material property of the plant leaves

3.2.1.2 Numerical simulation and topology optimization of the samples

LH65 WENZEL trilinear coordinates measuring instrument is used to measure the plant leaf data. In this study, only the coordinate data of the main vein and lateral vein in the setup system are measured, meanwhile the minor veins are ignored, considering that it plays an insignificant role in the mechanical performances. In order to build the mechanical model of leaf, the practical leaf structure is simplified. In practice, the cross section and thickness of the veins becomes smaller from the root (or the medial axis) to the tip (or the leaf rim). In this paper, the cross-section is hypothesized as round shape, and the outer diameter changes from the maximum to the minimum with linear function, whilst, the thickness keeps the same. The geometry model of leaves is built with the tool of ANSYS APDL Then, the model is imported to the commercial software Hypermesh to make the topology optimization. The target function is the minimum weighted compliance, and the constraint equation is volume fraction, which is set to be 0.3. In addition, the leaves are assumed to withstand loads from different directions, such as wind loads, rain and gravity. The topological optimum results are showed in Fig.11. The result gave an explanation that plant leaf vein is a kind of compliance effective structure with vein network pattern. A phenomenon was found by viewing all kinds of plant leaves in nature that different leaves growing in different conditions present various configurations, that is, the included angles between the major vein and lateral vein varied from 0° to 90° etc, while most of them varied in the range between 45° and 60°. What differs is the size of the cross section of the vein. Two main reasons cause the result, (1) in order to make the result less influenced by the error of numerical algorithm, the applied load is much bigger than the practical load that ordinary plants could withstand; (2) the reserved material based on the constraint condition in topology optimization is much more than the practical condition. Whereas, It is still deserved to notice that the material density is correlated with the load vector, that is, when the load takes place, the material appears where the stress needs, and the topology pattern of material elements corresponds well to the loading orientation, which explains that the mid axis pattern of plant vein is adaptive to the environmental stress. The main vein consistently remains unchanged, the lateral vein changes slightly along different load direction, which shows that the vein network of leaf has robust adaptability. The analysis shows that the plant leaf helps to keep the internal strain energy at a small value, and the environmental stress is one of the inducing factors for vein growth. It deserves to notice that the vein network of the plant leaf not only lends itself the physiological functions but also adapts to the complex environmental stress by evolving itself into a steady network pattern.

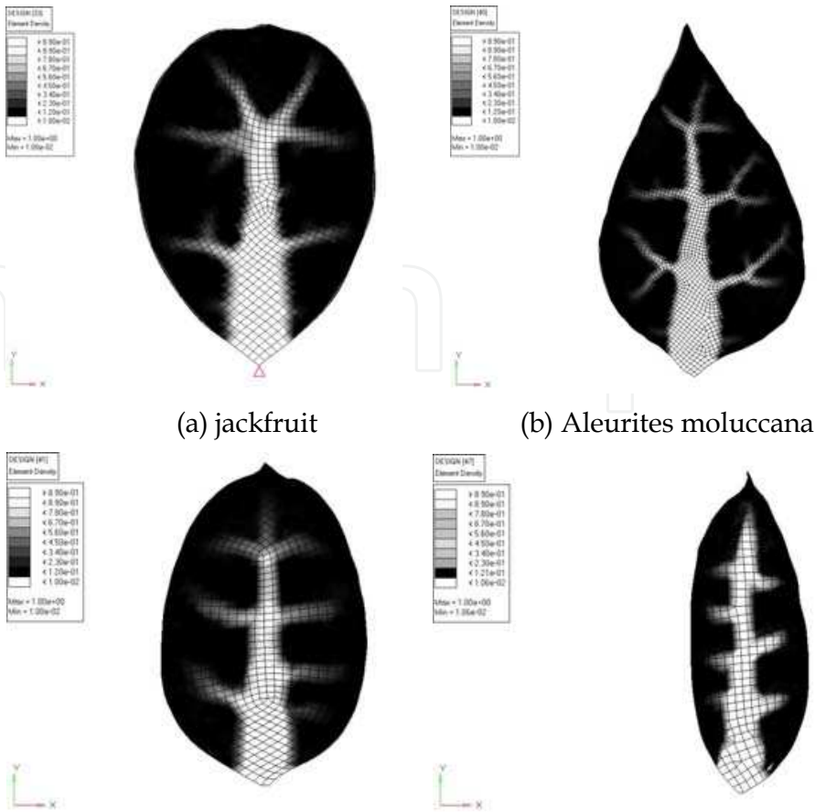

(a) jackfruit (b) Aleurites moluccana

(c) Ficus altissima (d) ficus viren

Fig. 11. The topology network of plant leaf

3.2.2 Adaptive blade design based on vein structure of plant leaf

The similarity between the plant leaf vein and the wind turbine blade can be explained as followings:

1. Structure and environment: both of the plant leaf and the blade are cantilever structure working in natural environment, and mainly suffer from wind load.
2. The Inner topology structure: the plant leaf has the principal vein and the lateral vein, and the lateral vein locates symmetrically at bi-lateral sides of the principal vein; Contrastively, large wind turbine blade is usually designed or configured as spanwise spar, a set of shear webs and composite skin structure, which is similar to the topology pattern of plant leaf. The design intention of large wind turbine blade is also obvious, that is, the spanwise spar is mainly used to carry the centrifugal force and the self weight, and the shear webs are used to carry the shear wind force.

It is not hard to see that the adaptive growth of plant leaf is driven by stress environment, and it can be used as a general guide to design wind turbine blade because of the similar working environment and structure requirement.

3.2.2.1 Blade optimization and bionic design for wind turbine

The baseline blade is originally developed by the institute of renewable energy research of Shan Tou University for 1.5 MW wind turbine, which is illustrated in Fig.12(a) (Xin, 2005). The length of the blade is 34m, and the airfoils are derived from Wortmann FX77/79Mod

airfoil series, where the first airfoil profile position begins at 8.15m from root part, whose detailed profile parameters and design operating case have been thoroughly documented by Han (2008). In order to prevent big deformation of blade tip from influencing the accuracy of calculation, the tip part is magnified slightly.

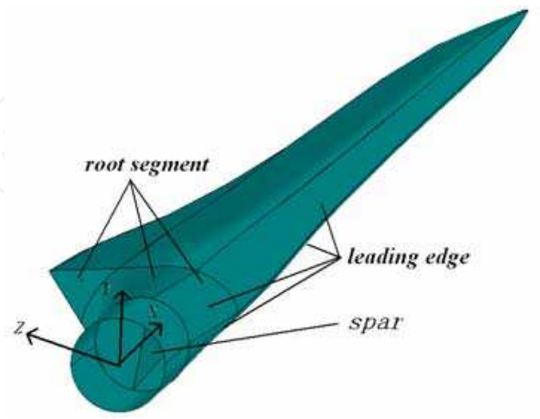

(a) The 1.5MW blade model and its key parts

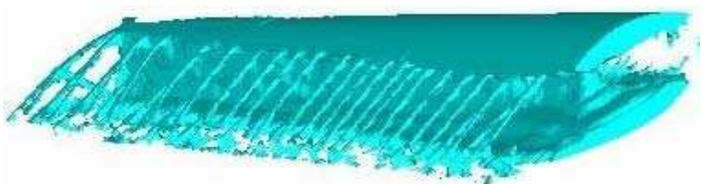

(b) Blade topology optimization result

Fig. 12. The model and topology optimization result of 1.5MW blade

We select the blade segment from 12 to 20m along the blade spanwise direction, and suppose this part is made of homogeneous material. The finite element model of the blade is established in HyperMesh, where, PSOLID elements and Solid Isotropic Material with Penalization (SIMP) method are used for structural topology optimization. The target function is the minimum weighted compliance, and the constraint equation is the volume fraction, which is set to be 0.3. Topological optimization results are shown in Fig.12(b) with the load of critical wind of 50 m/s and gravity. As shown in Fig.12(b), the blade topological structure suggests a rough impression of the blade material distribution, which are, the spar and web configuration. If the blade topology pattern compares with the plant leaf, much more clear impression could be achieved, shown as Fig.13. The blade spar cap and webs correspond to the main vein, and the blade skin corresponds to the lateral vein, which would change with the wind load direction.

It is of indubitability that the most adaptive structure in the world comes from natural design. The authors were highly inspired by the similar cantilever structure between plant leaf and wind turbine blades, as well as the similar stress environment. Therefore, it could be expected that wind turbine blade imitating the plant leaf structure could achieve the excellent adaptive performances. The authors main work mainly focus on the fiber orientation design imitating the plant leaf skeleton. As it is known that different plant leaves have different morphological structure and side vein angles, in order to explore which leaf skeleton pattern are more suitable for the performance requirement of wind turbine blades,

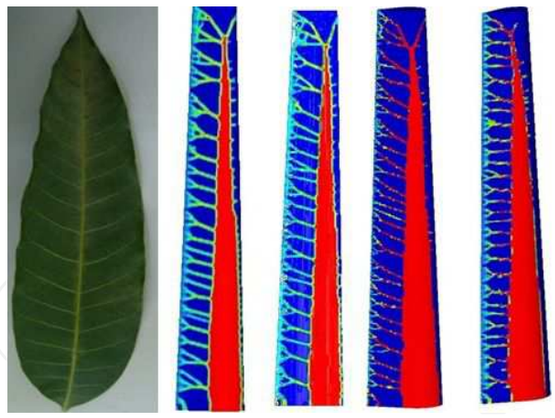

Wind directions in 30°, 45°, 60° and 90° , respectively

Fig. 13. Comparison of the topology structure between plants and turbine blade[]

different plying angles changed in the range of [0,90] are chosen to make the calculation of different performances. Referring literature, the particular angle 20° is specially considered. The main vein angles, calculated from the medial axis of the blade, are [10°/0°] (Liu et al., 2009). Traditionally, the stiffen spar is chosen as the coupled design region. Whereas, in our work, the design region is expanded to the skin part of the blade considering the leaf vein structure. First of all, the uncoupled e-glass blade with small modification is chosen as a baseline model for coupling structure design, which is illustrated in Fig.12. The parameters of the blades and material properties are listed in Table 3 (Hermann T & Locke).

Parameters	E-glass fiber/epoxy		T600 carbon fiber/epoxy		Foam
	Experiment	safety	Experiment	safety	
Flap module E11[GPa]	36.47	-	127.3	-	0.61
Radial module E12[GPa]	12.62	-	8.78	-	-
Shear module G12[GPa]	3.94	-	5.07	-	-
Possion ratio	0.22	-	0.24	-	0.2
Density [Kg/m3]	1880	-	1520	-	120
Tensile strain [%]	2.00%	0.82%	1.21%	0.49%	-
Compressive strain [%]	2.09%	0.85%	0.97%	0.40%	-
Shear stress F12[MPa]	62.5	25.5	73.6	30.04	-

Table 3. Material properties

Parameters	Baseline	Prototype	Error
weight(Kg)	5808	5800	0.10%
Tip deflection(m)	1.12	-	-
1st natural freq(Hz)	1.05	1.08	3.40%
2ndnatural freq(Hz)	1.87	1.82	2.70%
3rd natural freq(Hz)	3.8	3.39	12%

Table 4. Comparison between baseline blade and prototype

The baseline blade is made up of outer shells and two internal shear webs with the same width as the spar cap, which is designed as variable section, from 20% to 85% of spanwise direction, with thickness tapered via ply drops to reduce the blade weight, and the exterior skins and internal shear webs are both sandwich construction with triaxial fiberglass laminate separated by foam core, whose material property is shown in table 3. For the baseline model, the unidirectional glass fibers are used for uncoupling effect, and the shells are overlaid inside and out with bidirectional ±45° glass fabric normally.

The baseline blade, named as Model A, uses all glass/epoxy fibers shown in table 3. In order to examine if the baseline blade matches well with the prototype model chosen from document (Lobitz, 2000), the comparison is made by numerical simulation for the blade tip deflection under critical wind load and the previous two order natural frequencies. The results shown in table 4 indicate that the baseline model matches well with the prototype model, and only small deviations exist within the acceptable scope. It means that the approaches of modeling and simulating are accurate and practical.

In addition, two more configurations are built for bend-torsion coupling design. One is assumed to be the same as the baseline blade except that the unidirectional fibers in spar cap are replaced with T600 carbon material shown in table 3, named as model B; another model is adapted from model A except that the skin of the blade is replaced with T600 carbon fibers in order to make the effect of coupling.

3.2.2.2 Evaluation of performances considering different design models

Based on the blade FEM calculation method (McKittrick et al., 2001), the equations from (30) to (32) were used to calculate the coupling controlled factor and stiffness of each blade section (Griffin, 2002), whilst, If all the parameters of each section are used to evaluate the overall aerodynamic performances of the wind turbine blade, it is too complex and inconvenient to fulfill the evaluation. Literature (Wetzel, 2005) reported that the aerodynamic performances in the region closer to the blade tip are more important. Therefore, a full blade involved the equivalent coupling factor based on the weighted average result of each spanwise section could be established with the following formula:

$$\alpha^* = \frac{2}{Z_{tip}^2}\sum_{i=1}^{n}(\alpha_1 l_1 + \alpha_2 l_2 + \cdots + \alpha_i l_i) \tag{30}$$

where, z_{tip} is the overall length of the blade, α_i is the coupling factor of each section, l_i is the station of each section. Referring to this method, the full blade involved the equivalent flapping and torsion stiffness can be defined as：

$$EI^* = \frac{2}{Z_{tip}^2}\sum_{i=1}^{n}(EI_1 l_1 + EI_2 l_2 + \cdots + EI_i l_i) \tag{31}$$

$$GJ^* = \frac{2}{Z_{tip}^2}\sum_{i=1}^{n}(GJ_1 l_1 + GJ_2 l_2 + \cdots + GJ_i l_i) \tag{32}$$

The off-axis fibers orientation in the coupling region is the design variable. The random variable, namely the off-axis fiber angle in the coupling region, is supposed to follow the uniform distribution in the range of 0°~ 45°, because the related study shows that, when the

off-axis fibers angles change in the range of 0°~±45°, the best coupling effect can be obtained. 22 samples are randomly chosen, and the static and dynamic performances of the blade are evaluated for each change of the off-axis orientation. The static performance is achieved through 2 load steps in ANSYS. In the first step, the parameters of the blade working in flapping and torsion moment including the blade stiffness and the coupling factor are respectively calculated; In the second step, the stress and strain of the blade working at extreme wind speed 50m/s are calculated, including two groups of stress that play the main role in deciding the blade failure: one group involves the interlaminate shear stress and in-plane Von Mises stress; another group involves the maximum tensile strain and compressive strain. In the mean time, the dynamic performance is calculated to figure out the 1st out-of-plane and in-plane frequency. All the calculation job is realized with ANSYS random calculation module by the user-subroutine language APDL, and the results are shown in Fig.14, Fig.15 till Fig.19.

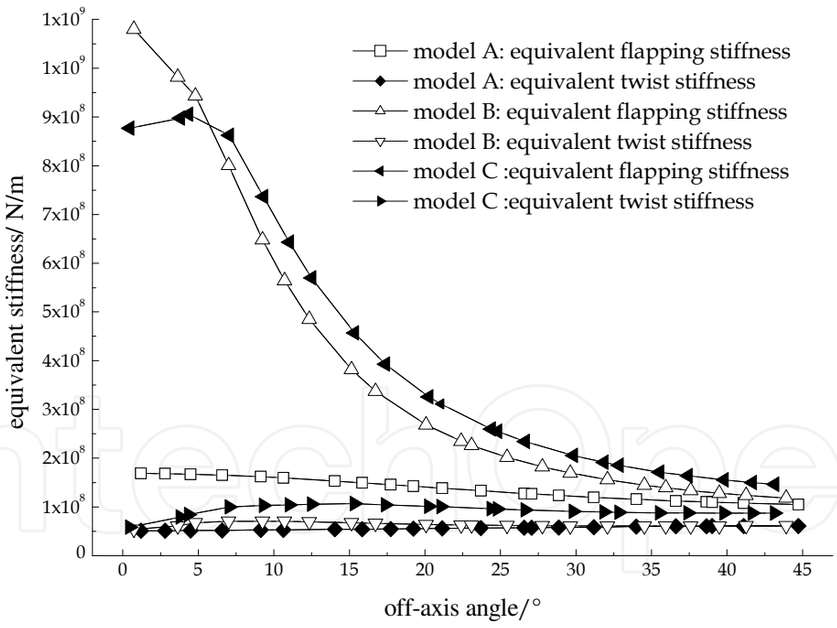

Fig. 14. The equivalent flapping and torsional stiffness

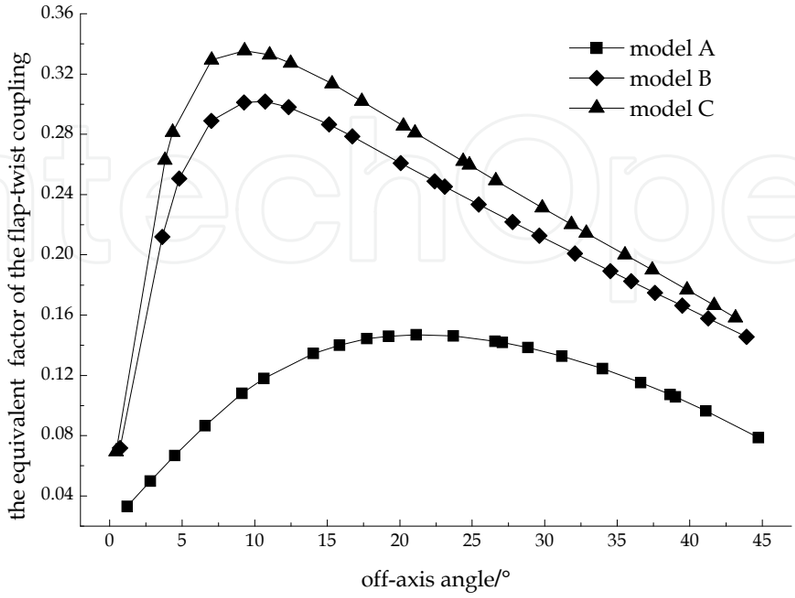

Fig. 15. The equivalent coupling factor –torsion

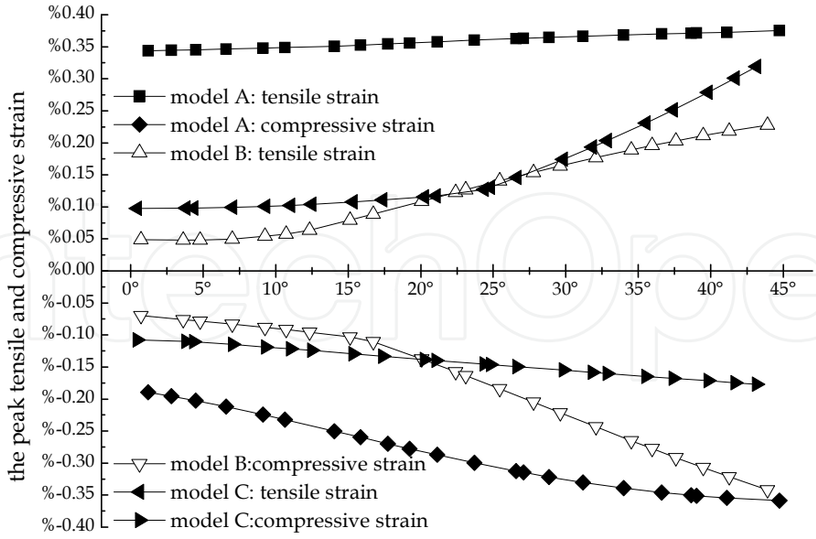

Fig. 16. The peak fibers tensile and compress strain

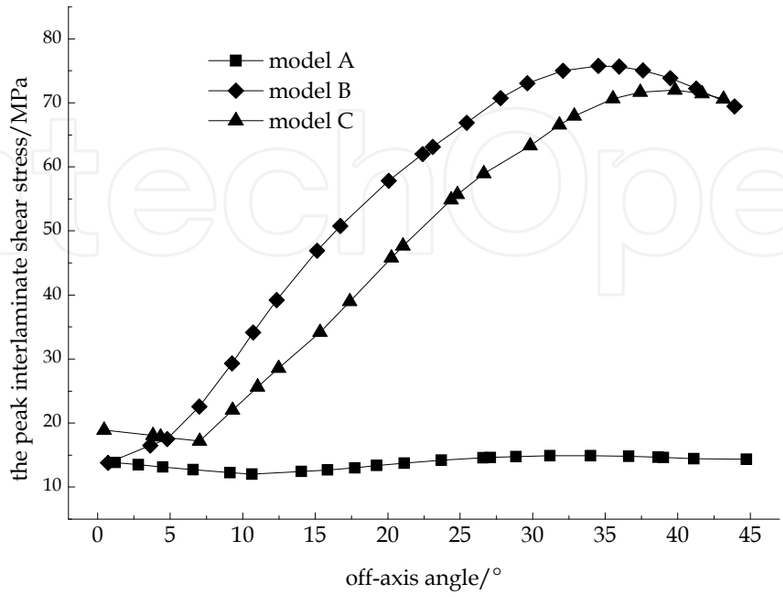

Fig. 17. The interlaminar shear stress

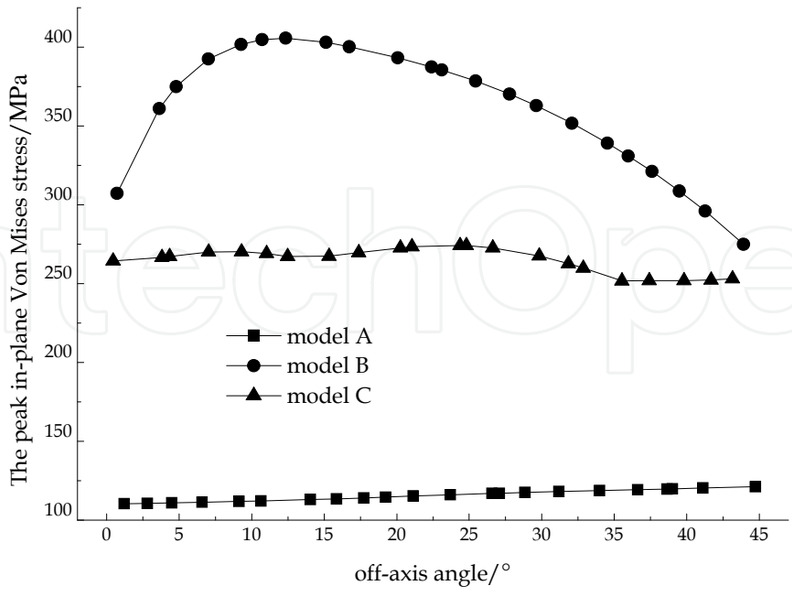

Fig. 18. The in-plane Von Mises stress

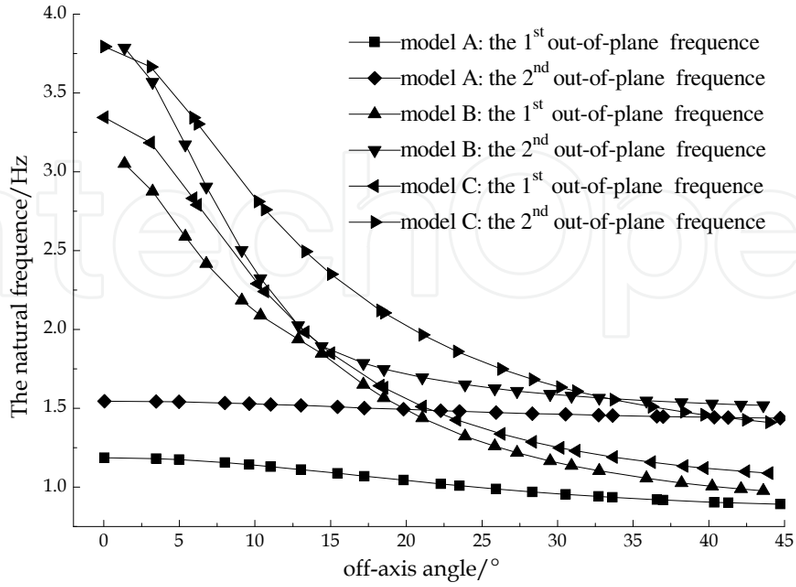

Fig. 19. The natural frequence

It can be observed from Fig.14 that, the overall trend of the equivalent flapping stiffness of each model is decreased with the increase of off-axis angle. Because the carbon fibers axial module is several times of the glass fibers, the flapping stiffness of model B and model C will be proportionally increased other than model A near 0°. But obviously, the carbon fibers axial module is dramatically decreased with the increase of the off-axis angle, which leads to the rapid decrease of the flapping stiffness. Comparatively, the torsion stiffness of the 3 models have little difference. The result achieved in paper (Liu &Zhang, 2010b) accords well with the theory introduced in the context, and it also agrees well with the result in the literature mentioned before. Meanwhile, it validates that the definition of the equivalent parameters in previous section is reasonable.

It can be known from Fig.15 that model B and model C achieve better coupling effect than model A, and off-axis fibers in blade skin achieve better coupling effect than off-axis spar cap. The off-axis angle which generates the maximum coupling effect of the three models is also different. The off-axis angle of model B and model C is about 11°, whereas, model A is about 20°. In addition, it is clear that, near the off-axis angle which achieves the maximum coupling effect, the flapping stiffness is still large. From this point, the spar thickness or the skin thickness can be also reduced so as to reduce the blade weight.

It can be observed from Fig.16 that the maximum tensile and compressive strains are increased with the increase of off-axis angle. The reason is that the decrease of the flapping stiffness leads to the increase of the deflection, which results in the increase of the corresponding tensile and compressive strain. Therefore, the fibers volume fraction and off-axis angle should ensure that the strains are within the safe range. It can be deduced that, when the glass fibers are replaced with carbon fibers, if the designed stiffness is expected to be equivalent with the reference stiffness, it can be reduced by diminishing the layer thickness. As the maximum compressive strain of carbon fibers is smaller than that of glass

fibers, it should be careful not to make the tensile and compressive strain of carbon fibers exceed the safe value. The blade structure in this chapter is not exactly equal to the practical blade, and all the tensile and compressive strain do not exceed the safe range.

In Fig.17, it can be observed that the interlaminate shear stress is increased considerably with the increase of off-axis fiber angle in model B and model C. It climbs to about 74MPa, which is close to the dangerous situation for the carbon fibers used in this chapter. Large interlaminate shear stress will increase the possibility of transverse breakage of the interlaminate fibers if it exceeds the reference value. Definitely, it also becomes an important factor to constrain the blade design.

In Fig.18, it can be observed that the maximum in-plane Von Mises stress for model A has a small increasing trend with the increase of off-axis angle. Before 15°, there is an obvious decrease for model B, then decrease rapidly. Whereas, for model C, we can see the peak in-plane stress drops with the increase of angle in a way of slight fluctuation. According to the cumulate principle of Palmgren Miner's fatigue damage, low in-plane stress would be helpful to increase the blade fatigue life. In this sense, model B and model C may not be good to achieve longer fatigue life. Actually, this phenomena is caused by the properties of material itself. If the models are made up of the same material, and the coupling design is achieved only through regulating the off-axis fibers arrangement, it is found that the model imitating the compliant structure of plant leaf has better fatigue performances(Liu & Zhang, 2010a)

It can be known from Fig.19 that, the first order frequency of the out-of-plane and in-plane are all decreased with the increase of off-axis angle in three models. This is because the blade natural frequency is proportional to its stiffness, especially for model B and model C. The decline trend of the natural frequency is much more dramatically owing to the rapid drop of the stiffness, but carbon fibers can highly raise the natural frequency, which can be clearly seen that the design stiffness for model B and model C are always higher than that of the baseline blade. Therefore, it will not influence the dynamic performance of the blade.

3.2.3 Adaptive blade design based on stress trajectory

It is well known that in fiber reinforced composites, the fibers take the main function of carrying the load, and the matrix takes the function of bonding material and spreading the stress. Thus, it is commonly acceptable and understandable to match the fiber orientation with the principal stress orientation. Following this thought, at each point in the structure, three orthogonal sets of fibers, each subjected to an essentially uni-directional load, would carry all of the three principal stresses by utilizing the immense longitudinal strength and stiffness of the fibers. As fibers are orientated with the three principal stresses, the further advantage for a composite component is that it leads to minimal secondary stresses in the resin (Liu & Platts, 2008).

Wind turbine blades are critical components carrying the bending and torsional moment caused by wind and other force source. The general failure mode of wind generator is fatigue failure happened on some fracture-critical components in wind turbine system. Using ANSYS APDL and the special composite element Shell99, a 1.5MW wind turbine blade model, whose data was originated from (Li et al., 2005), was created and shown as Fig.12. The principal stress field in different wind load cases was processed, and the streamlines of the principal stress are shown in Fig.20(a)-(c), plotted with the shadow lines.

It can be observed from Fig.20(a)-(c) that when the incoming wind flow is perpendicular to the blade windward surface, the streamlines of the principal stress would go along with the

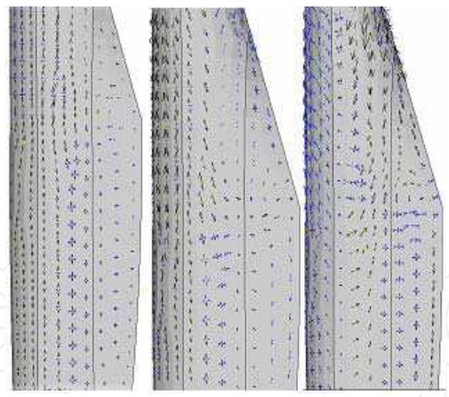

(a)0° (b)45° (c)-45°

Fig. 20. The blade principal stress field distribution

blade span direction; When the incoming flow is tilted to the blade windward surface and the rotational axis or rotational plane, the streamlines of the principal stress would change their orientation according to the force source change. Usually, the blade is made of GFRC (or CFRC) in UD(Unidirectional) type(the volume ratio could be 7:1) and lateral type(the volume ratio could be 1:1), where the UD plies carry most of the bending moment and centrifugal force, and the lateral plies bear most of the torsional moment and shearing force. In practice, the orientation of the incoming flow changes continuously, which leads to the principal stress field in the blade change homologous. This kind of complex stress environment requires that the blade material could be able to adapt to the change of the principal stress field in order to make use of its maximum loading effect. According to the similar working environmental analysis and similar structural requirement, the adaptive topology structure of plant leaf could be used as a guide to design a kind of adaptive blade structure. Traditionally, the blade plying orientations are usually 0° and 45°, whereas, according to medial axis pattern of plant leaf, the newly designed blade plying orientation are 0°, 22.5°, 45° and 67.5°, where, the angles are defined as the included angles between the UD plies and the lateral plies. Two kinds of 1.5MW blade model were designed in different plying orientations, and their dynamic and static performances are analyzed. Complying with the IEC61400– 1999 standards, the random wind field mode was taken as the random load sample, and the wind velocity complies with Weibul distribution, whose shape parameter is 2 and the scaling parameter is 15. The incoming flow orientation is regarded as uniform distribution. Now supposing two kinds of blades are working in the same wind field mode mentioned above, and the Monte Carto sampling method in ANSYS was used to calculate the blade performances. According to the change trend of the standard deviation for output values specified, 200 samples are reasonable. The maximum Von Mises stress and the standard deviation for traditional type and medial axis type are listed respectively as followings: 2.5594MP_a, 2.5750MP_a; 2.4631MP_a, 2.4007MP_a; It denotes that the maximum stress of the modified medial axis type is less discrete and more stable than the traditional one, which is helpful to improve the blade fatigue lifetime.

3.2.4 Material design of the blade

The length and weight of the blade would be considerably increased with the increase of power capacity of individual wind turbine generator. The confliction between power

increase and blade length and weight increase leads to the problem that GFRP can not fully meet high performance requirement of the large-scale blade(>50meters). Instead, lightweight CFRP with high performance becomes the trend of blade material application. Whereas, high cost of CFRP makes it impossible to fully use it in the whole blade. Therefore the application of hybrid composites of GFRP and CFRP in large and medium-sized blades becomes the development trend.

According to design methods of large-scale blades, usually the airfoil leading edge and spar should be taken as the key design regions because of carrying the most moment, and at the same time the root segment of the blade where stress concentration easily appears also becomes focus of attention, especially for large-scale seashore wind turbines which are liable to be damaged from the roots caused by torsional vibration in typhoon. Therefore, the general guideline is to add a small amount of carbon fibers in the leading edge, spars and root segment of the blade to improve its comprehensive performance.

Taking the 1.5MW blade as an example, the model and each key part is defined as Fig.12, the material used is listed in Table 5.

Material	E1(MP_a)	E2(MP_a)	G12(MP_a)	ν	ρ (Kg/m^3)
GFRP(7:1)	42600	16500	5500	0.22	1950
GFRP(1:1)	17500	17500	3600	0.14	1950
CFRP(7:1)	142500	24200	10170	0.24	1580
CFRP(1:1)	26500	26500	8600	0.15	1580
Urethanefoam	60.8	59.8	19.18	0.20	119.7

Table 5. Material mechanical properties

The blade performance is discussed considering the following cases.

Case 1. the analysis results of prototype model in document (Liu & Platts, 2008), which only have the frequency values.

Case 2. the model used above in this article. Which exists somewhat inaccuracy compare with prototype model.

Case 3. based on Case2, 2mm CFRP (7:1) layers are added in leading edge as UD laminates.

Case 4. based on Case3, 2mm CFRP (1:1) layers are added in leading edge as lateral laminates.

Case 5. based on Case4, 2mm CFRP (1:1) layers are added in spar sandwich structure.

Case 6. based on Case5, 2mm CFRP (7:1) layers are added in root segment.

In Case 3, 5 and 6, each CFRP laminate locates at the same layer.

40m/s wind speed in the wind field site is taken as the extreme load, and a series of computations considering above cases were carried out with ANSYS. Fig.21 shows the results of dynamic performance, where the first-order waving and second-order swing natural frequency were obtained, the sixth torsional frequency, which has significant effect on the blade torsional vibration. Fig.22 shows the static performance, where the maximum displacement and Von Mises stress is obtained.

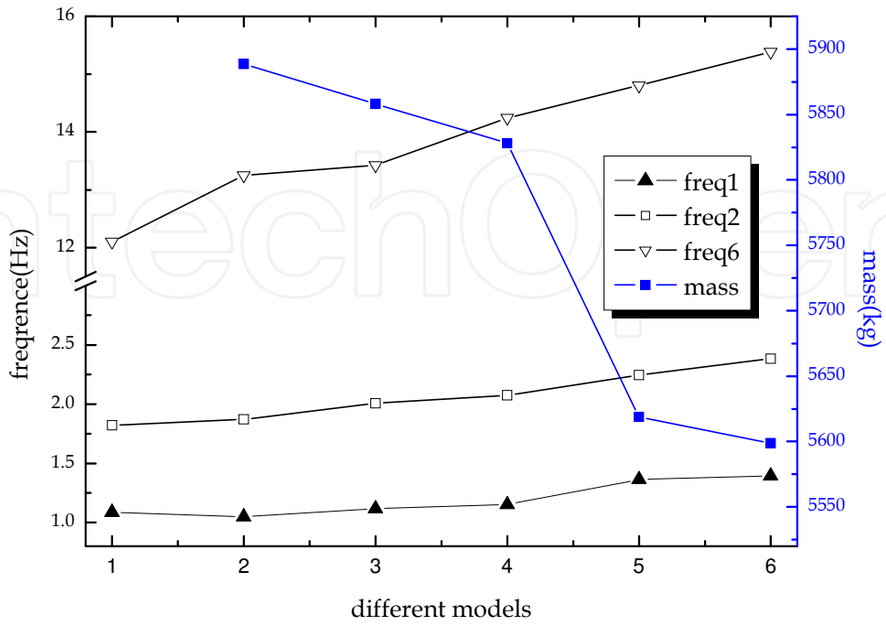

Fig. 21. The dynamic performance in different cases

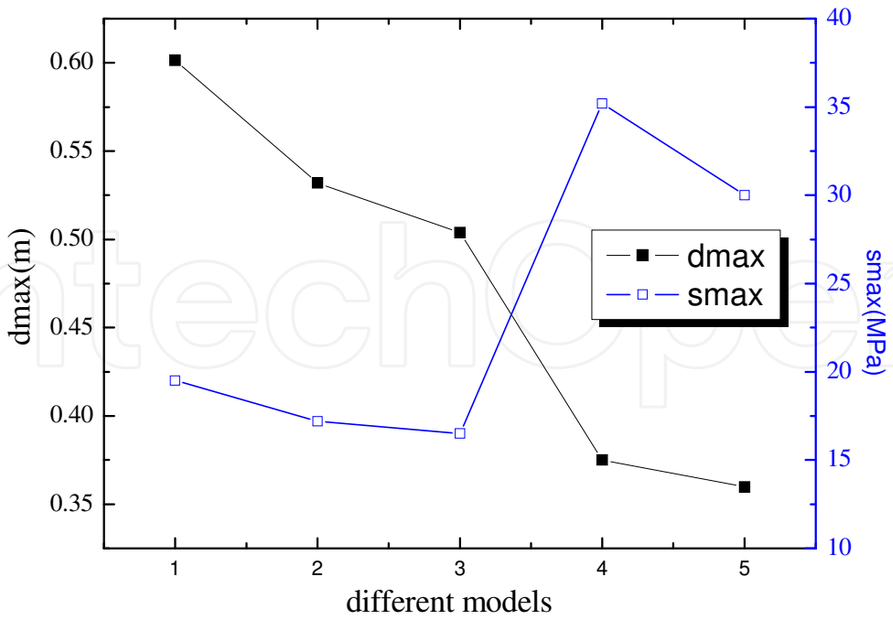

Fig. 22. The static performance in different cases

In Fig.21, number 1-6 on the X-axis represent Cases 1-6, and number 1-5 in Fig.22 represent cases 2-6. It can be observed from the figures that when the CFRP in the leading edge is added, and then in spar, and root segment in turn, each order frequency can be improved obviously and the blade weight was reduced. The blade tip displacement becomes smaller, but Von Mises stress becomes greater with the increasing of CFRP amount. These can be explained as followings, where:

$$\omega = \sqrt{\frac{K}{I}} \tag{33}$$

$$\sigma = E\varepsilon \tag{34}$$

In formula (33), *K*, *I* represent stiffness coefficient and inertia of the blade. It is obvious that the frequency ω is in direct proportion to *K*. Formula (34) shows that stress σ will increase with *E*. Whereas the strain ε is in inverse proportion to *EI*, which was named as bending stiffness in the spar theory. Here, *K* and *E* become bigger as the CFRP is added, and the frequency ω and stress σ increase at the same time.

Above all, when hybrid composites are utilized in the blade, the dynamic performance can be improved and the deformation and the weight of the blade can be reduced. Whereas, the stress will increase unavoidable. Necessary measures must be taken to balance the contradictory, which needs further study.

4. Conclusion

In this chapter, the design and evaluation of adaptive blade based on tend-torsion coupling effect is explored, incorporated the bionic design method from the flexible topological structure of plant leaf. Three models for coupling design are built referring to a 1.5MW baseline blade. The investigations on parametric design for off-axis fiber angle of the coupled blade are conducted respectively. The results show that, the glass/carbon hybrid fibers are the best choice for coupling design, which can provide high coupling coefficient between 15°~25° of off-axis fiber angles, rather than single glass fibers. For the three models, the maximum tensile and compressive strain and stress increase with the increase of off-axis fibers angle, whereas, the in-plane stress in hybrid fiber blades decreases. It is recommended to place the fibers before 25° to ensure the blade structure safety. Following that, a kind of bionic design method is integrated into the coupled blade design, and the result shows that it can improve the blade bend-torsion coupling effect further.

5. Acknowledgement

The authors are thankful to the support of national natural science foundation of China (the Grant No. 50675067 and 50975090).

6. Reference

Simon Philippe Breton & Geir Moe. (2009). Status, plans and technologies for offshore wind turbines in Europe and North America. *Renewable Energy*. 34, pp. 646-654.

N W M Bishop & L W Lack, L Li. (1999). Analytical fatigue life assessment of vibration induced fatigue damage. *IPENZ Transactions*. 26, pp. 1-17.

Knut O Ronold, Jakob Wedel-Heinen & Carl J Christensen. (1999). Reliability-based fatigue design of wind-turbine rotor blades. *Engineering Structure*. 21, pp. 1101–1114.

Knut O Ronold & Gunner C Larsen. (2000). Reliability-based design of wind-turbine rotor blades against failure in ultimate loading. *Engineering Structures*. 22, pp. 565–574.

Christoph W Kensche. (2006). Fatigue of composites for wind turbines. *International Journal of Fatigue*. 28, pp. 1363–1374.

Daniel D Samborsky, et al. (2008). Delamination at Thick Ply Drops in Carbon and Glass Fiber Laminates Under Fatigue Loading. *Journal of Solar Energy Engineering*. 130, pp. 1-8.

Raif Sakin & Irfan Ay. (2008). Statistical analysis of bending fatigue life data using Weibull distribution in glass-fiber reinforced polyester composites. *Materials and Design*. 29, pp. 1170-1181.

Don W. Lobitz & Paul S. Veers. (1998). Eroelastic Behavior of Twist-Coupled Hawt Blades. *American Institute of Aeronautics and Astronautics*. AIAA-98-0029, pp. 1-9.

Bao N S, et al. (2007). Dynamic characteristics of large-scale stall wind turbine system. *Acta Energiae Solaris Sinica*. 28(12), pp. 1329-1334.

Lin Y G. (2005). Study on the Technology of Pitch-control for Large Scale Wind Turbine. Doctor Dissertation. Zhejiang, Zhe Jiang University.

Matthew A Lackner & Gijs A M. van Kuik. (2010). The Performance of Wind Turbine Smart Rotor Control Approaches During Extreme Loads. *Journal of Solar Energy Engineering*. 132, pp. 1-8.

Andreas Büter & Elmar Breitbach. (2000). Adaptive blade twist calculations and experimental results. *Aerosp. Sci. Technol* . 4, pp. 309–319.

Karaolis N M, G Jeronimidis & P J Musgrove. (1989). Composite Wind Turbine Blades: Coupling Effects and Rotor Aerodynamic Performance, *EWEC'89, European Wind Energy Conf*, Glasgow, pp. 10-13.

Joosse, P. A. & R. M. van den Berg. (1996). Development of a TenTorTube for Blade Tip Mechanisms, Part 1: Feasibility and Material Tests, Proc, *European Union Wind Energy Conf. and Exhib*, GF6teborg, pp. 20-24.

Andrew, T.L & Richard, G. J. (1999). The compliant blades for wind turbines. *IPENZ Transactions*. 26, pp. 7 -12.

Don W. Lobitz, et al. (2001). The Use of Twist-Coupled Blades to Enhance the Performance of Horizontal Axis Wind Turbines. SAND 2001-1303.

Ladean R. McKittrick, Douglas S. Cairns, & John Mandell. (2001). Analysis of a Composite Blade Design for the AOC 15/50 Wind Turbine Using a Finite Element Model. SAND 2001-1441.

Dayton A Griffin & Thomas D Ashwill. (2003). Alternative composite materials for megawatt-scale wind turbine blades: design considerations and recommended testing. *Wind Energy*. 125, pp. 515-521.

Mansour H Mohamed & Kyle K Wetzel. (2006). 3D Woven Carbon/Glass Hybrid Spar Cap for Wind Turbine Rotor Blade. *Journal of Solar Energy Engineering*. 128, pp. 562-573.

John F. Mandell, Daniel D. Samborsky & Lei Wang. (2003). New fatigue data for wind turbine blade materials. *Wind Energy*. 125, pp. 506-514.

J Selwin Rajadurai, et al. (2008). Finite element analysiswith an improved failure criterion for composite wind turbine blades. *Forsch Ingenieurwes*. 72, pp. 193–207.

James Locke & Ulyses Valencia. (2004). Design Studies for Twist-Coupled Wind Turbine Blades[R]. SAND 2004-0522.

Dayton Griffin. (2002). Evaluation of Design Concepts for Adaptive Wind Turbine Blades[R]. SAND2002-24 24.

Kyle. K Wetzel. (2005). Utility Scale Twist-Flap Coupled Blade Design. *Journal of Solar Energy Engineering*. 127, pp. 529-537.

Alireza Maheri, Siamak Noroozi & Chris A Toomer. (2006). WTAB, a computer program for predicting the perfor-mance of horizontal axis wind turbines with adaptive blade. *Renewable Energy*. 31, pp. 1673–1685.

Alireza Maheri, Siamak Noroozi & John Vinney. (2007). Application of combined analytical FEA coupled aero structure simulation in design of wink turbine adaptive blades. *Renewable Energy*. 32, pp. 2 011-2018.

Alireza Maheri & Askin T Isikveren. (2009). Design of Wind Turbine Passive Smart Blades, *European Wind Energy Conference*, France.

Alireza Maheri & Askin T. Isikveren. (2009). Performance prediction of wind turbines utilizing passive smart blades: approaches and evaluation. *Wind Energy*. (in press)

Rachel F Nicholls-Lee, et al. (2007). Enhancing Performance of a Horizontal Axis Tidal Turbine using Adaptive Blades, *OCEANS 2007 Europe*, UK, pp. 1-6.

R F Nicholls-Lee, S W Boyd & S R Turnock. (2009). Development of high performance composite bend-twist coupled blades for a horizontal axis tidal turbine, *17th International Conference on Composite Materials* , UK.

Jim Platts & W Y Liu. (2008). Developing Chinese Wind Energy Technology, *Young Scholars Symposium for Design and Manufacture of New Energy of National Natural Science Foundation*, Guangzhou.

Crawford Curran & Platts Jim. (2006). Updating and optimization of a coning rotor concept. Collection of technical papers, *44th AIAA Aerospace Science Meeting*, Reno, Nevada, 10, pp. 7265-7280.

Crawford Curran. (2006). Re-examination the precepts of the blade element momentum theory for coning rotors. *Wind Energy*. 9(5), pp. 457-478.

Sarikaya M, Gunnison K.E & Yasrebi M. (1990). See shells as a natu-ral model to study laminated composites, *Lancster Penn sylvania: Tech Pub Co Inc*, pp. 176-183.

Gordon J E, Jeronimidis G. M & O W Richardson. (1980). Composites with high work of fracture. *Mathematical and Physical Sciences*. 294,1411(A), pp. 545- 550.

Steele C R. (2000). Shell stability related to pattern formation in plants. *Journal of Applied Mechanics*. 67(2), pp. 237-247.

Somerville Chris, Bauer Stefan & Brininstool Ginger. (2004). Review: Toward a system approach to understanding plant cell Walls. *Science*. 306(24), pp. 2206-2211.

S E Jones & M J Platts. (1998). Practical Matching of Principal Stress Field Geometries in Composite Components, *97 International Conference on Automated Composites*, Oxford, Elsevier, 29, pp. 821-828.

Blum H & Nagel R. (1978). Shape description using weighted symmetric axis features. *Pattern Recognition*, 10(3), pp. 67-180.

W Y Liu, et al. (2007). Relationship between medial axis pattern of plant leaf and mechanics self-adaptability(I): experimental investigation and numerical simulation. *Journal of South China University of Technology: Natural Science Edition*, 35(3), pp. 42-46.

W Y Liu, J X Gong, W F Hou. (2009). Relationship between medial axis pattern of plant leaf and mechanics self-adaptability(II): vein structures with different vector angles and topological pattern of plant leaf. *Journal of South China University of Technology: Natural Science Edition*, 37(8), pp. 12-16.

Y Q Jiang, F S Lu & Gu Z J. (1990). *Mechanics of Composite Materials*, Xi'an Jiaotong University Press, Xi'an .

Cheng Huat Ong. (2000). Composite wind turbine blades. Doctor Dissertation. *Stanford University*, USA.

Cheng Huat Ong & Stephen W Tsai. Design, manufacture and testingofa bend-twist spar. SAND99-13.

Lornal J. Gibson & Michael F. Ashby. (1997). Cellular solids: structure and properties, *Cambridge university press*, England.

W Y Liu & Y Zhang. (2010a). Network study of plant leaf topological pattern and mechanical property and its application, *The 3rd International Conference of Bionic Engineering*, Zhuhai

W P Xin. (2005). Analysis of dynamic characteristics and response for rotating blades of wind turbine, Master Dissertation , *Shantou University*, China.

Xinyue, Han. (2008). Muti-objective optimization design and structure dynamic analysis of HAWT blade, Master Dissertation, *Shantou University*, China.

W Y Liu, J X Gong, & W F Hou. (2009). Relationship between medial axis pattern of plant leaf and mechanics self-adaptability (II): vein structures with different vector angles and topological pattern of plant leaf. *Journal of South China University of Technology (Natural Science Edition)*. 37, pp. 12-16.

Hermann T & Locke J. (2005). Failure Analysis of Anisotropic Laminate Composites *Utilizing Commercial FEA Software*. in: AIAA-2005-0975 (2005), pp. 370–381.

W Y Liu & Y Zhang. (2010b). Bend-Twist Coupling Design and Evaluation of Spar Cap of Wind Turbine Compliance Blade, *International Conference on Manufacturing Engineering and Automation 2010*, Guangzhou. (in press)

W Y Liu & M . J. Platts, (2008). Concept representation, practical topology decision and analysis in composites lug design, *ICFDM*, Tianjin, 8, pp. 636-643.

D Y Li, Z Q Ye, & Chen Y. (2005). Mutli-body dynamics numerical analysis of rotating blade of horizontal axis wind turbin. *Acta Energiae Solaris Sinica*. pp. 475-781.

W Y Liu, J X Gong & X F Liu. (2009). A kind of innovative design methodology of wind turbine blade based on natural structure.in: Information and Computing Science, *ICIC '09. Second International Conference*, Manchester, England ,pp. 350-354.

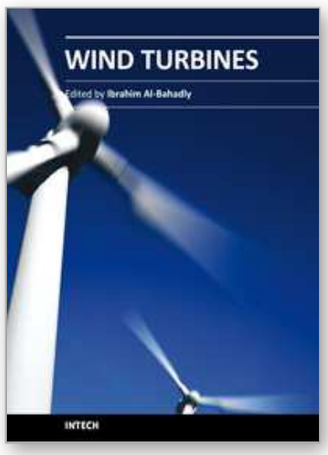

Wind Turbines

Edited by Dr. Ibrahim Al-Bahadly

ISBN 978-953-307-221-0
Hard cover, 652 pages
Publisher InTech
Published online 04, April, 2011
Published in print edition April, 2011

The area of wind energy is a rapidly evolving field and an intensive research and development has taken place in the last few years. Therefore, this book aims to provide an up-to-date comprehensive overview of the current status in the field to the research community. The research works presented in this book are divided into three main groups. The first group deals with the different types and design of the wind mills aiming for efficient, reliable and cost effective solutions. The second group deals with works tackling the use of different types of generators for wind energy. The third group is focusing on improvement in the area of control. Each chapter of the book offers detailed information on the related area of its research with the main objectives of the works carried out as well as providing a comprehensive list of references which should provide a rich platform of research to the field.

InTech Europe
University Campus STeP Ri
Slavka Krautzeka 83/A
51000 Rijeka, Croatia
Phone: +385 (51) 770 447
Fax: +385 (51) 686 166
www.intechopen.com

InTech China
Unit 405, Office Block, Hotel Equatorial Shanghai
No.65, Yan An Road (West), Shanghai, 200040, China
中国上海市延安西路65号上海国际贵都大饭店办公楼405单元
Phone: +86-21-62489820
Fax: +86-21-62489821

IntechOpen